Geomechanics and Engineering, *Vol. 29, No. 3 (2022) 259-267*
https://doi.org/10.12989/gae.2022.29.3.259

Penetration behavior of biopolymer aqueous solutions considering rheological properties

Jae-Eun Ryou[a] and Jongwon Jung*

Department of Civil Engineering, Chungbuk National University, 1 Chungdae-ro, Seowon-gu, Cheongju-si, Chungcheongbuk-do, Republic of Korea

(Received December 21, 2021, Revised February 25, 2022, Accepted March 3, 2022)

Abstract. The rheological and penetration characteristics of sodium alginate and xanthan gum aqueous solutions were analyzed for the development of biopolymer-based injection materials. The results of viscosity measurements for the rheological characteristics analysis show that all aqueous biopolymer solutions exhibit a tendency for shear-thinning, i.e., the apparent viscosity decreases as the shear rate increases. In addition, a regression analysis using several models (Power-law, Casson, Sisko, and Cross) was applied to the shear-thinning fluid analysis results, the highest accuracy was determined by applying the power-law model. The micromodel experiment for the penetration characteristics analysis determined that all biopolymer aqueous solutions show higher pore saturation than water, and that pore saturation tends to increase as the flow rate and concentration increases. When comparing the rheological and penetration characteristics of the biopolymer aqueous solution used in this study, the xanthan gum aqueous solution showed a fully developed shear-thinning tendency, unlike the sodium alginate aqueous solution. This tendency is considered to have the advantage of enhancement injectability and pore saturation.

Keywords: biopolymer; penetration characteristics; pore saturation; shear-thinning fluid flow; viscosity

1. Introduction

Recently, the use of underground space and soft ground has gradually increased in order to supplement the low availability of construction sites and efficiently secure urban spaces. Ground improvement is necessary for an efficient use of underground spaces and soft ground, and various ground improvement methods such as loading, substitution, dehydration, and grouting methods have been conducted. Among them, the grouting method has the advantage of being free from restrictions regarding the selection of the target area, which has little effect on adjacent structures and underground facilities, and does not lose its effectiveness in the flow of groundwater when the density of the hardening material is high. The grouting method can also be applied to improve the bearing capacity of a foundation, prevent water ingress during tunnel excavation, prevent piping during excavation, and prevent a reduction in the groundwater level. In addition to improving the ground strength and expanding the water resistance, the grouting method is also applied to reduce ground deformation, fill pores and cracks, and expand the foundations of structures and restore uneven settlements. Although the injection technology using cement as an injecting material has improved and been widely used, it has the disadvantage that it cannot be used in injections targeting cracks in a rock with a large amount of leakage and gaps, as the penetration of cement particles is small. For this reason, research on the development of grout injection methods with alternative materials has been conducted. A new injection material was invented by adding calcium chloride as a coagulant to water glass, which was the beginning of the chemical injection method. From then on, the development of new grout materials using water glass as the main material continued. However, water glass grout has problems in terms of strength and durability, and to compensate for these problems, it is used in parallel with cement-based grout and polyurethane (Karol 2003, He *et al*. 2016, Zhang *et al.* 2018). Unlike water glass-based grouting, polymer-based grouting may show advantages in strength and durability depending on the type of injection material. In addition, micro-cement and polymer-based grouts with small particle diameters were used to reinforce microcracks, but in the case of micro-cement, clogging occurred due to the formation of filter cakes, whereas in the case of polymer-based injection materials, the injection showed a relatively stable pattern (Jeoung *et al.* 2016, Hwang *et al*. 2018). However, polymer-based grouting is typically polyamide-based, or polyurethane-based, and amide-based grouting is prohibited owing to its unique toxicity. Therefore, the development of an eco-friendly polymer-based biopolymer injection material could be an excellent alternative.

In this study, fundamental research on the applications of an aqueous biopolymer solution grout was performed. Viscosity measurements were performed for rheological analysis and micromodel experiments for the penetration characterization. In addition, the experimental results were comparatively analyzed according to the type and concentration of the biopolymer.

*Corresponding author, Associate Professor
E-mail: jjung@chungbuk.ac.kr
[a]Ph.D. Student
E-mail: jaeeunryou@chungbuk.ac.kr

ISSN: 2005-307X (Print), 2092-6219 (Online)

2. Previous studies

2.1 Biopolymers

As the importance of environmental issues emerged, eco-friendly ground improvements started receiving considerable attention (Zhou *et al.* 2020). A biopolymer is a biodegradable material whose origin is a natural material produced by the cells of an organism. Biopolymers are being applied in various fields, such as the food industry, packaging, manufacturing, and medicine. Biopolymers used for ground improvement are diverse, such as xanthan gum, agar gum, guar gum, β-glucan, casein, chitosan, and sodium alginate. A representative ground improvement via biopolymer soil treatment leads to increased strength and reduced permeability.

The permeability reduction effect of biopolymer treatments was analyzed according to curing time, soil type, and biopolymer type (Bouazza *et al*. 2009, Taytak *et al*. 2012, Wiszniewski and Cabalar 2014, Ayeldeen *et al.* 2016, Lee *et al*. 2021). As the curing time increased, the reduction of permeability coefficient decreased because the soil particle-polymer link weakened with time (Wiszniewski and Cabalar 2014). Through comparison of the conducted studies, no clear trend could be found in the reduction of the permeability coefficient according to the type of soil and the type of biopolymer, suggesting a limitation in the quantitative evaluation due to the small number of comparable studies.

Studies on uniaxial compressive strength and shear strength have been conducted in various ways, such as on biopolymer type and concentration, soil type, and durability (Amelian *et al.* 2022, Chang and Cho 2014, Chang *et al.* 2015a, Chang *et al.* 2015b, Chang and Cho 2019, Kumar and Sujatha 2021). It has been reported that the uniaxial compressive strength increases according to the concentration of xanthan gum in the biopolymer, and that the strength increase is higher for clay soil, which is due to the matrix formed by the ionic and hydrogen bonds between clay particles. (Chang and Cho 2019, Cheng and Geng 2021).

The effect of biopolymer treated soil is strength enhancement and permeability reduction, controlling soil erosion resistance, preventing desertification, restoring ground, and enhancing oil recovery (Jung and Ahn 2014, Jung *et al.* 2016, Jang *et al*. 2017, Lee *et al*. 2017, Fatehi *et al.* 2018, Ham *et al*. 2018, Park *et al.* 2020, Ko and Kang 2020). The intended applications for biopolymers in geotechnical engineering can vary such as the use of pavement and earth stabilization, vegetation growth promotion (Chang *et al*. 2020).

2.2 Viscosity

Viscosity refers to the fluid property of resisting the flow and is an important factor in determining the flow pattern of fluids in pores. The viscosity of a fluid can be used to determine the viscosity number and the capillary number, which evaluate the type of injection patterns such as viscous fingering and capillary fingering (Lenormand and Zarcone 1989, Jung *et al.* 2014, Cao *et al*. 2016a, Cao *et al.* 2016b). In addition, the viscosity of an injected fluid is a direct factor that influences the fracture type and volumetric flow rate into the ground.

An apparent viscosity of aqueous biopolymer solution depends on the shear rate, and the aqueous biopolymer solution is considered as a non-Newtonian fluid. The behavior of non-Newtonian fluids can be induced by several factors and is typically related to the structural reorganization of fluid molecules due to flow. The rheological results differ depending on the type and concentration of the biopolymer, and it is difficult to determine a non-Newtonian fluid or not with the given data. For an aqueous biopolymer solution containing sodium alginate and xanthan gum, the shear stress tends to increase non-linearly as the shear rate increases, which can be considered as shear thinning. Non-Newtonian fluid models for shear-thinning fluid analysis include the Power-law, Casson, Sisko, and Cross models.

The power-law model expresses the shear properties of a fluid, which can be derived from the relationship between the shear rate and the logarithmic value of the apparent viscosity (Ostwald 1929). Apparent viscosity is defined as the ratio of the shear stress to the shear rate, and the power-law model can be applied to shear-thickening fluids, for which the shear stress increases nonlinearly as the shear rate increases. Among the parameters of power-law, the flow behavior index N represents the behavior of the fluid. If the N value is less than 1, it indicates shear-thinning. If it is greater than 1, it indicates shear-thickening. And if it is 1, it indicates a Newtonian fluid. The consistency index, K, is obtained by regression analysis. The Casson model describes the relationship between the square root of the shear stress and the yield stress of the fluid, and the Casson viscosity and shear rate. It has the characteristic of a gradual change between the Newtonian fluid region and the yield region such that it is mainly utilized to describe the flow of viscoelastic fluids (Casson 1959). The Sisko model is a fluid model that considers the shear rate, shear stress, and apparent viscosity, and is typically applied to lubricants and greases (Sisko 1958). The Cross model explains the pseudoplastic flow of a fluid without yield stress because of the relationship between the initial apparent viscosity and the infinite apparent viscosity (Cross 1979). The equations for each model are shown in Table 1.

In this study, the non-Newtonian fluid model of a biopolymer aqueous solution was determined through regression analysis of the power-law, the Casson, Sisko, and Cross models, which are representative models of shear-thinning fluids.

3. Materials and methods

The biopolymers used in the preparation of the injection material were sodium alginate and xanthan gum, which were in powder form. An aqueous solution was prepared by mixing them with water in a predetermined weight ratio. The weight ratios were 0.5% to 2% for sodium alginate, and 0.1% to 0.4% for xanthan gum. A hot plate with a magnetic stirrer was used to maintain a temperature of 70 °C for 24 h.

Table 1 Non-Newtonian rheological models of shear-thinning fluid

Rheological model	Equation	Model parameter
Power-law	$\tau = k\dot{\gamma}^N$	τ: shear stress
Casson	$\sqrt{\tau} = \sqrt{\tau_0} + \sqrt{k\dot{\gamma}}$	τ_0: shear stress at zero rate
Sisko	$\tau = \mu\dot{\gamma} + k\dot{\gamma}^N$	k: consistency index
Cross	$\mu = \mu_\infty + \frac{\mu_0 - \mu_\infty}{1 + k\dot{\gamma}^N}$	N: flow behavior index
		μ: apparent viscosity
		μ_0: apparent viscosity at zero rate
		μ_∞: apparent viscosity at infinite rate

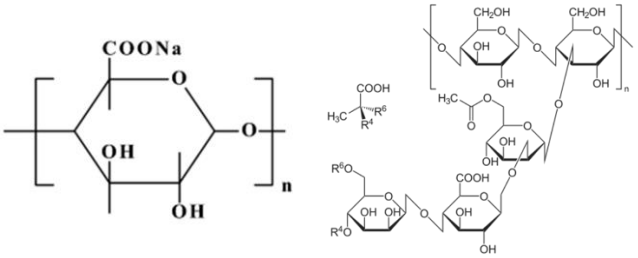

(a) Sodium alginate (b) Xanthan gum

Fig. 1 Chemical structures of the biopolymers

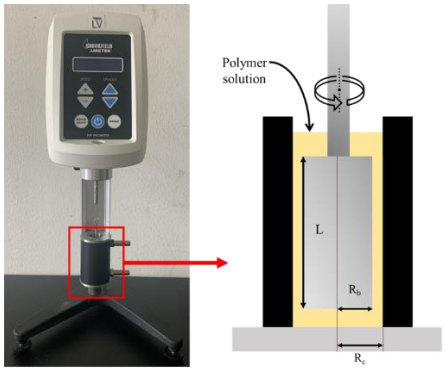

Fig. 2 Experimental devices for viscosity measurement

Thereafter, viscosity measurements were performed to determine the flow characteristics of the aqueous biopolymer solutions by type and concentration. Micromodel injection experiments were performed for a penetration characteristics analysis.

3.1 Materials

Sodium alginate (Sodium alginate, MP Biomedicals, LLC) and xanthan gum (Xanthan gum, Sigma-Aldrich, 43708) were both present in powder form, and their chemical structures are shown in Fig. 1.

Sodium alginate is composed of mannuronic acid and L-glucuronic acid, which exists in the form of a gel with high elasticity or high hardness depending on its concentration. Owing to these viscoelastic properties, it is also used in heavy metal adsorption, food, and the pharmaceutical industries. Sodium alginate is also used as an inexpensive substitute for industrial materials (Pathak *et al*. 2008). The effect of ground improvements using sodium alginate is an increase in the recovery modulus for subgrade soil, which increases the shear modulus and damping ratio. This is due to an increase in the binding force due to cross-linking between sodium alginate and the soil particles (Arab *et al*. 2019, Ahn *et al*. 2020). Xanthan gum is produced by the bacterial species Xanthomonas campestris. The uniaxial compressive strength and shear strength of the soil can be increased through soil improvements with xanthan gum treatment (Chang *et al*. 2015a, Chang *et al*. 2015b, Soldo and Miletic 2019). In addition, a xanthan gum aqueous solution exhibits a characteristic, whereby the structure changes depending on the dissolution temperature and brine concentration. As the concentration of xanthan gum increases, it shows a high stability across various temperature and pH ranges (Chang *et al*. 2014, Butler 2016). Viscosity was measured according to the concentrations of the sodium alginate and the xanthan gum powder.

Brookfield viscometer (LV-DVE) is used to measure the viscosity of the biopolymer aqueous solution (see Fig. 2). Shear resistance was measured by selecting a spindle suitable for the viscosity of the solution according to the type and concentration of the biopolymer. A spindle provided a constant rotation of between 1 and 50 rpm which is related flow rate. The viscosity measured in the range of shear rate 1-40 (1/s). The viscosity and shear stress according to the shear rate were calculated using the measured shear resistance and RPM.

3.3 Micromodel experiment

The micromodel injection experiment consisted of a fluid injection device, a micromodel, and an image analysis equipment. As the fluid injection device, a syringe pump (Syringe pump, KatsScientific, NE-1010) capable of controlling the injection speed of distilled water (DI) and the biopolymer aqueous solution and a filter for removing foreign substances were used. The micromodel (micromodel, micronit, uniform network) was created by superimposing two symmetrical silicon dioxide (SiO_2) glass plates, whereby the width and length of the glass plates were 10 mm and 20 mm, respectively. The micromodel consisted of 576 disk-shaped particles. A disk-shaped particle can be used to simulate the surface characteristics of a ground soil particle, and with the region between the disk-shaped particles indicating the pores, and the pores present at each position being adjacent to three different pores. The diameter of disk-shaped particle is 590 μm. The diameter of the circular pore body is 61.56 μm and the throat length is 32.94 μm. A dark room and a high-resolution camera were used as image analysis equipment

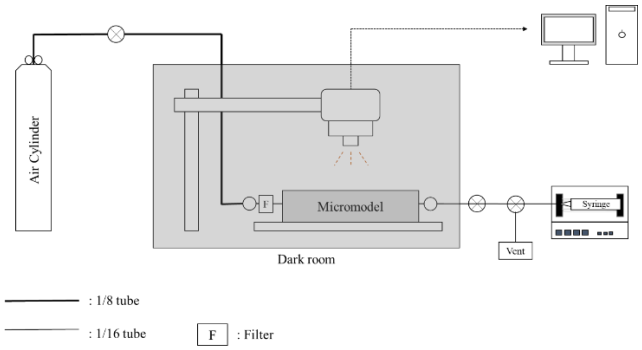

Fig. 3 Schematic diagram of the micromodel test

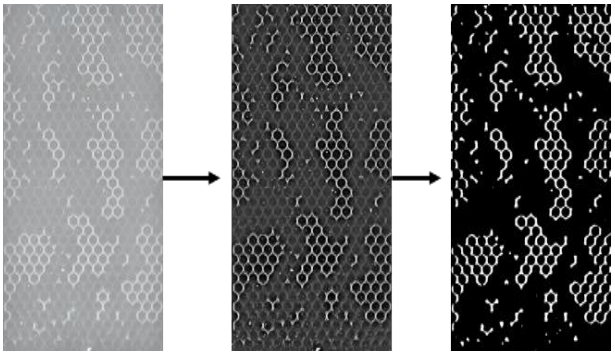

Fig. 4 Processes of image treatment including thresholding and binarization

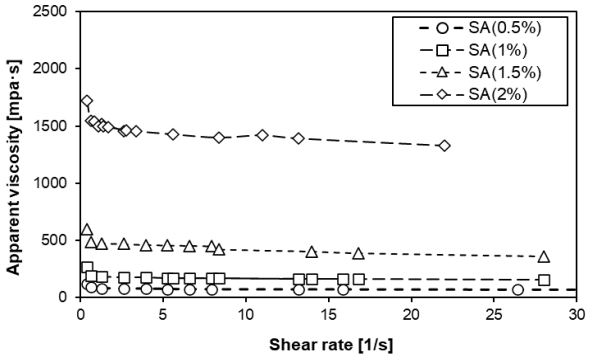

(a) Sodium alginate

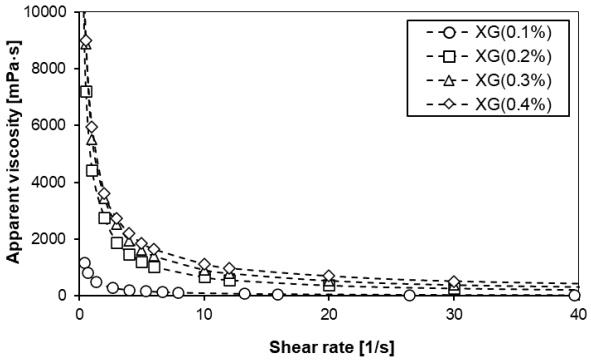

(b) Xanthan gum

Fig. 5 Apparent viscosity changes with shear rate

for analyzing the pore saturation of the micromodel according to the injection amount of the biopolymer aqueous solution. A dark room was used to reduce the error caused by brightness during image processing, and the injection pattern in the micromodel was analyzed using a high-resolution camera. For the micromodel injection experiment, the biopolymer aqueous solution was filled into a syringe, and then the DI and biopolymer aqueous solution were injected into the micromodel according to the desired flow rate using a syringe pump. Thereafter, the pore saturation of the aqueous biopolymer solution in the micromodel was calculated using a high-resolution camera.

The micromodel injection experiment was performed on pores filled with air, and the injection was continued until no change could be observed in the pores due to the injected solution. Before each experiment was performed, ethanol was injected to wash the fluid injection tube and micromodel to minimize the experimental error caused by any remaining foreign matter. The volumetric flow rates of the syringe pump were 1, 10, 100, and 1000 μL/min to analyze changes in pore saturation. A schematic of the overall micromodel injection experiment is shown in Fig. 3.

The original image obtained by the micromodel injection experiment requires image processing because there are brightness errors due to the light of the image. The image processing method converts the original image into an 8-bit gray image, specifies the range of the minimum and maximum pixels through filtering, and calculates the ratio of the binary residual fluid and the injected fluid through thresholding to determine the pore saturation. ImageJ software and an image processing code were used for image processing, and the entire process is shown in Fig. 4.

4. Experimental results

The apparent viscosity change with shear rate are measured. A suitable non-Newtonian model for the biopolymer aqueous solution is determined by regression analysis. The micromodel injection results show pore saturations according to biopolymer type and concentration.

4.1 Apparent viscosity

Results show the apparent viscosity as a function of the shear rate (see Fig. 5). The apparent viscosity of both sodium alginate and xanthan gum aqueous solutions decreases with the increase in the shear rate, which presents the shear-thinning. In addition, as the concentration increased, the apparent viscosity at the same shear rate tends to increase. The sodium alginate aqueous solution have an apparent viscosity of 67.2 to 120, 158.2 to 270, 360 to 650, and 1330 to 1720 mPa·s at concentrations of 0.5, 1, 1.5, and 2%, respectively. The xanthan gum aqueous solution has concentrations of 0.1, 0.2, 0.3 and 0.4%, with the apparent viscosity values ranging from 41.4 to 1170, 114.6 to 7200, 165 to 11000, and 243.6 to 12600 mPa·s, respectively. While apparent viscosity of the aqueous solution of sodium alginate a little decreases, the xanthan gum aqueous solution shows a tendency for a rapidly decreasing apparent viscosity according to the shear rate. In addition, the xanthan gum aqueous solution has a relatively low concentration compared with the sodium alginate but has a relatively large apparent viscosity value due to its high molecular weight.

Table 2 R^2 values by the regression analysis using Power-law, Casson, Sisko, and Cross models

Biopolymer	Concentration [%]	Power-law	Casson	Sisko	Cross
Sodium alginate	0.5	0.9968	0.3775	0.9331	0.8752
	1	0.9999	0.5633	0.8983	0.8406
	1.5	0.9991	0.3298	0.7150	0.8317
	2	0.9997	0.4231	0.9950	0.9878
Xanthan gum	0.1	0.9906	0.9000	0.9943	0.9727
	0.2	0.9834	0.9282	0.9978	0.9718
	0.3	0.9914	0.9183	0.9899	0.9817
	0.4	0.9981	0.9739	0.9975	0.9730

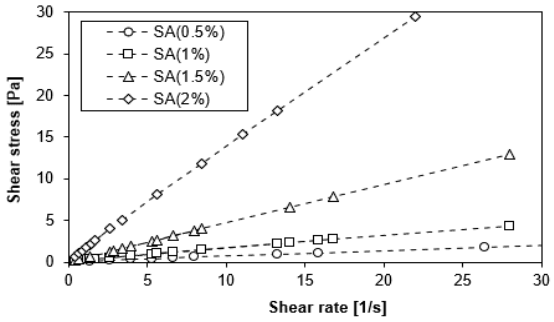

(a) Sodium alginate

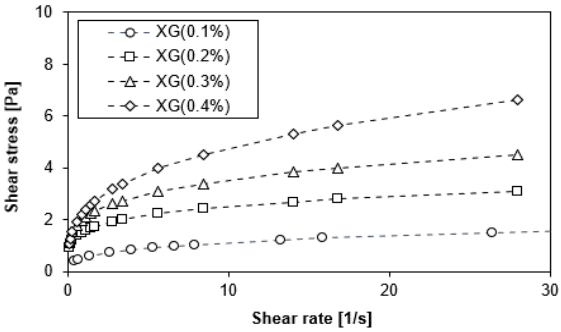

(b) Xanthan gum

Fig. 6 Rheological flow curve of biopolymer solutions

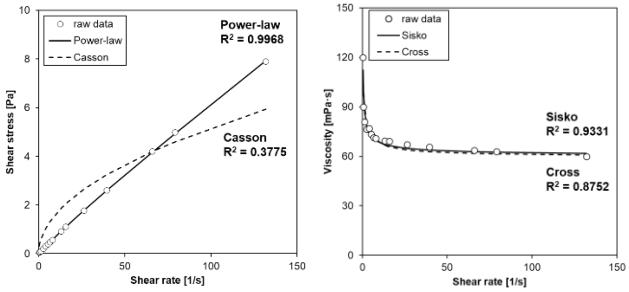

(a) Power-law and Casson (b) Sisko and Cross

Fig. 7 Determination of non-Newtonian model

Rheological flow curve of biopolymer aqueous solutions is shown in Fig. 6. As the shear rate increases up to 30 (1/s), the shear stress increases at all concentrations. The ranges of the shear stresses of the sodium alginate aqueous solutions are 0–2, 0–4, and 0–12 for concentrations of 0.5, 1, 1.5, and 2%, respectively. Also, when the concentration of the xanthan gum aqueous solution is 0.1, 0.2, 0.3, and 0.4%, the shear stress ranges show 0-1, 0-2, 0-4, and 0-7 Pa, respectively. Both solutions show increasing shear stress values with concentration for the same shear rate.

The shear stress of the xanthan gum aqueous solution is higher than sodium alginate at the given shear rate. For example, comparing the 0.5% sodium alginate aqueous solution and the 0.4% xanthan gum aqueous solution, the shear stresses are 1.2 Pa and 6 Pa, respectively at the same shear rate of 20 (1/s). The sodium alginate aqueous solution can be seen as Newtonian fluid because of linearly increases of shear stress according to shear rate. However, as the apparent viscosity decreases with the shear rate, it is clearly a shear-thinning fluid (see Fig. 5(a)). In contrast, in the case of the xanthan gum aqueous solution, the value of the shear stress increases nonlinearly as the shear rate increases, exhibiting a typical shear-thinning pattern.

4.2 Non-Newtonian model

The example of the regression analysis for determining the non-Newtonian fluid model of the aqueous biopolymer solution is shown in Fig. 7. All biopolymer aqueous solutions tend for shear-thinning, and regression analysis is performed using four representative models of shear-thinning, i.e., Power-law, Casson, Sisko, and Cross, to analyze the rheological properties of the fluid. While the power-law shows the highest R^2 value, the Casson model shows the lowest R^2 value that is more suitable for a viscoelastic fluids with yield stress. R^2 values of the Sisko and Cross models are 93% and 84%, respectively. In the case of the Sisko and Cross models, a high range for the shear rate and infinite apparent viscosity values are used as input values. Therefore, it means that the power-law and Sisko are the most suitable model for the sodium alginate and xanthan gum, respectively (more details are provided in Table 2).

The change in the power-law parameters according to the type and concentration of the aqueous biopolymer solution is shown in Fig. 8. The K value ranges from 0.086 to 1.5839 for sodium alginate and from 0.5728 to 2.3462 for the xanthan gum aqueous solution. The two biopolymer aqueous solutions exhibit an increasing K value with increasing concentration. The K value of xanthan gum aqueous solution increases rapidly according to concentration and for sodium alginate solution, the K value increases steadily under 2% concentration. The N value of

Table 3 Results of regression analysis of power-law parameters according to the concentration of the sodium alginate and xanthan gum aqueous solutions

Biopolymer	Concentration [%]	N (Flow behavior index)	K (Consistency index)
Sodium alginate	0.5	0.9266	0.086
	1	0.9486	0.1877
	1.5	0.9836	0.4889
	2	0.9456	1.5839
Xanthan gum	0.1	0.2884	0.5728
	0.2	0.1948	1.577
	0.3	0.2357	2.06
	0.4	0.3	2.3462

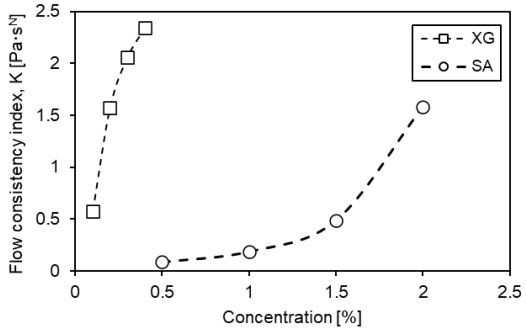

(a) Flow consistency index

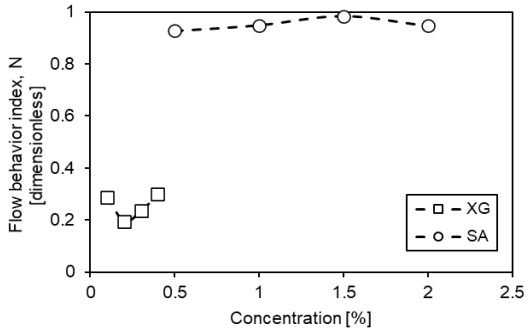

(b) Flow behavior index, N

Fig. 8 Power-law parameters according to biopolymer type and concentration

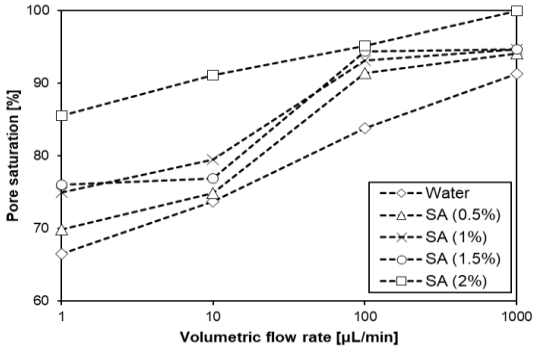

(a) Sodium alginate

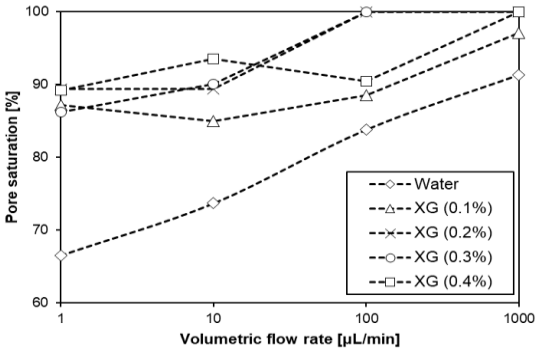

(b) Xanthan gum

Fig. 9 Pore saturation changes with volumetric flow rate

the sodium alginate aqueous solution is in the range between 0.9266 and 0.9836 and for xanthan gum aqueous solution it is between 0.1948 and 0.3. The N value of the power-law parameter indicates the nonlinearity of the fluid. When the value of N is 1, the fluid is classified as a Newtonian fluid, and when it is not 1, it is classified as a non-Newtonian fluid. In particular, the aqueous solutions of sodium alginate and xanthan gum exhibits shear-thinning behavior. The power-law parameters K and N tend to be affected by the type and concentration of the biopolymer, respectively (more details are provided in Table 3).

4.3 Micromodel test

The results of the micromodel injection experiment are shown in Fig. 9. The pore saturation of water increases with the volumetric flow rate. All biopolymer aqueous solutions exhibit an increase in pore saturation according to the concentration, which is due to the difference in viscosityratio between the residual fluid (water) and the injection fluid (biopolymer solutions) as the viscosity increases. In all biopolymer aqueous solutions, the pore saturation tends to increase as the volumetric flow rate increases. This is because the pressure increases with an increase in the volumetric flow rate into pores of the same volume.

For a sodium alginate concentration of 0.5–1.5%, the pore saturation in each flow rate are similar values up to 1000μL/min. Also, the huge increase of pore saturation occurs between 10 and 100 μL/min. It implies less influence of a sodium alginate concentration up to 1.5% on the pore

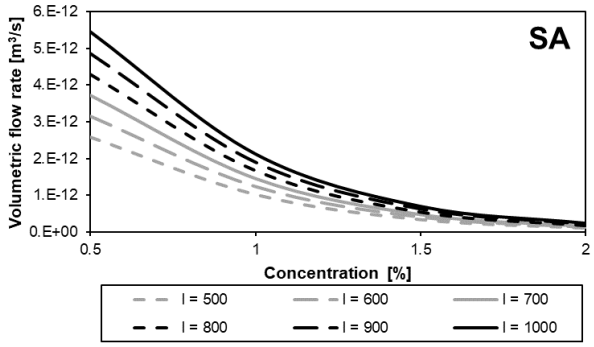

(a) Sodium alginate

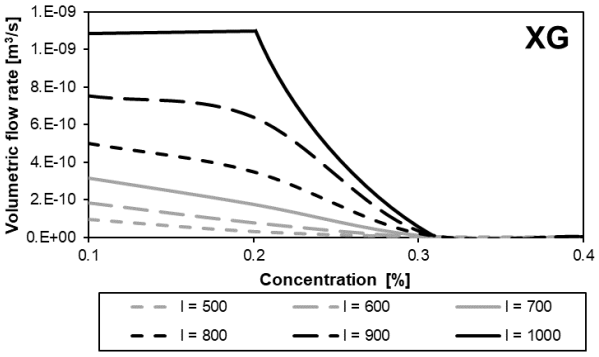

(b) Xanthan gum

Fig. 10 The effect of biopolymer aqueous solutions on volumetric flow rate

saturation than 2%. In the case of 2%, the result shows the clear increase of pore saturation with the concentration. Compared with the sodium alginate aqueous solution, the results of xanthan gum aqueous solution show a pore saturation of 85% or more at a volumetric flow rate of 1 μL/min. Thus, no clear increase of pore saturation is shown up to 10 or 100 μL/min. For example, the 0.1% and 0.4% xanthan gum concentrations show similar pore saturation up to 100 μL/min. Finally, when the flow rate is 1000 μL/min, the pore saturation becomes at least 97.07%.

5. Discussions

5.1 Effect of power-law parameters on flow characteristics

The volumetric flow rate in pores of biopolymer aqueous solution can be estimated using a modified Hagen-Poiseuille equation Eq. (1), which depends on the injection pressure, flow length, pore size, flow behavior index, and flow consistency index (Sochi 2010).

$$Q = \frac{N\pi}{3N+1}\left[\frac{\Delta P}{2KL}\right]^{\frac{1}{N}} R^{\frac{3N+1}{N}} \quad (1)$$

Where Q is volumetric flow rate(L/min), N is flow behavior index(dimensionless), $\triangle P$ is pressure gradient (Pa), K is flow consistency index(Pa·s^N), L is flow length(m), R is pore radius(m).

The pore radius and length are assumed to be 30, 300 μm, which are considered as the pore size of sandy sediment (Spariharijaona *et al*. 2019). In addition, the hydraulic gradient is ranged from 500-1000 to describe the high pressure condition.

The volumetric flow rate of sodium alginate and xanthan gum aqueous solutions is shown in Fig. 10. The volumetric flow rate increase as the hydraulic gradient increases. On the other hand, the volumetric flow rate decrease as the concentration increases. In both cases, as the concentration increases, K increases but N shows similar values (Table 3). Thus, Fig. 10 implies that the flow rate decreased due to the increase of K value.

The volumetric flow rate change according to the type of the biopolymer shows a different trend which is related to the N value. In the case of sodium alginate, N has the range of 0.9266-0.9836, which is closed to N value of Newtonian fluids i.e., N=1 and results in a sharp decrease in low concentration. However, for the xanthan gum, N values are relatively low (N=0.1948-0.3), which results in a similar flow rate until 0.2% concentration. It implies that xanthan gum aqueous solution is more available to increase volumetric flow rate at a low concentration.

5.2 Invading patterns of biopolymer aqueous solutions

Fig. 11 shows the invading patterns of the immiscible fluid flow. The injection of a biopolymer into air-saturated ground results in an air-biopolymer system, which is part of the flow of the immiscible fluids. Viscosity and capillary number affect the invading patterns of the immiscible fluids (Lenormand and Zarcone 1989). The viscosity number is indicated by M and is defined as the ratio of the viscosity of the invading fluid to that of the defending fluid. The capillary number refers to Ca and is affected by the viscosity, surface tension, contact angle, and flow rate of the invading fluid. The viscosity of the injection fluid is calculated using minimum and maximum values. As a result of analyzing the penetration patterns of sodium alginate and xanthan gum aqueous solution, assuming that the flow rate is the same, both fluids are found to belong to the range necessary for a stable displacement. In the case of sodium alginate aqueous solution, the M value is higher than that of water, but the Ca value shows a similar trend. Xanthan gum aqueous solution showed a more stable trend than water due to an increase in the M and Ca values. Due to this trend, it seems that the pore saturation for xanthan gum is the highest. In conclusion, the relative invading pattern of a biopolymer aqueous solution can be inferred through the calculation of the viscosity and the capillary number, but an experimental study on the surface properties of the aqueous biopolymer solution and air is required for a quantitative comparison of the invading patterns.

6. Conclusions

In this study, fundamental study was conducted on the flow and penetration characteristics of injection materials,

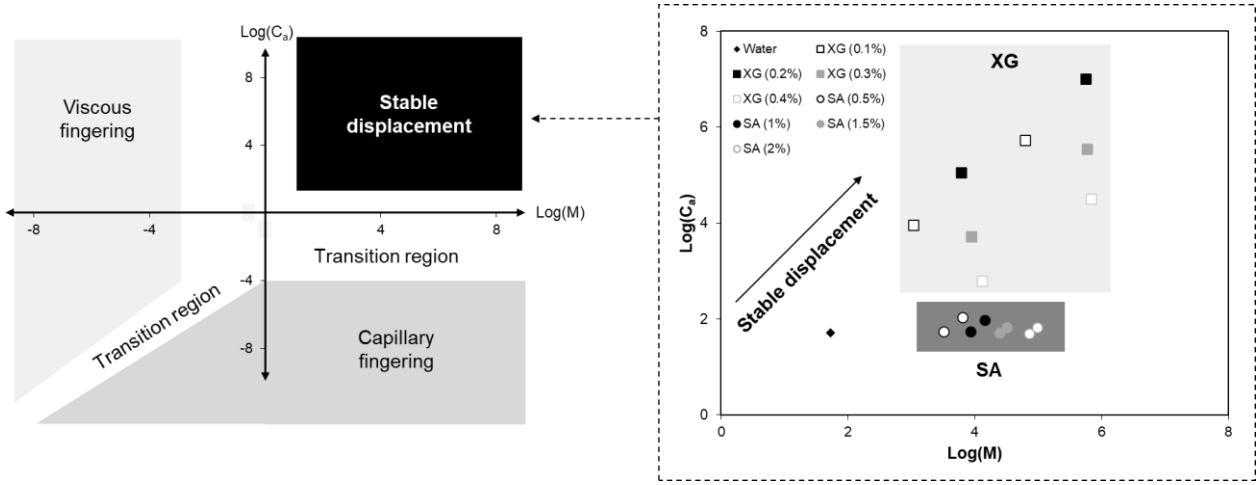

Fig. 11 Invading patterns of biopolymer aqueous solution-air system

i.e., of sodium alginate and xanthan gum aqueous solutions. Flow characteristics were analyzed by measuring the viscosity of the biopolymer aqueous solution of each type and concentration, and the penetration characteristics were analyzed through micromodel injection experiments. The conclusions of this study are as follows:

• Aqueous solutions of biopolymers show a tendency for shear-thinning, in other words, the apparent viscosity decreases as the shear rate increases. In the case of sodium alginate, the shear stress increased relatively linearly as the shear rate increased, and in the case of xanthan gum, the behavior of a typical shear-thinning fluid could be shown.

• Based on the results of a regression analysis on the representative models of shear-thinning, the highest accuracy was shown for the power-law model. In the power-law parameter analysis, the xanthan gum aqueous solution showed a significantly lower N value compared with sodium alginate, and both biopolymers showed a tendency for an increasing K value as the concentration increased.

• The biopolymer aqueous solution shows a higher pore saturation value with increasing concentration. Xanthan gum aqueous solution shows a higher pore saturation than sodium alginate aqueous solution at similar concentrations and volumetric flow rates because of high viscosity number.

• Compared to the Newtonian fluid, the shear-thinning fluid has a sharply changed volumetric flow rate according to the pressure gradient. These properties indicate the fluid which has a low flow behavior index can have advantages for high pressure grouting.

• The pore saturation of the injection fluid is affected by the injection pressure. However, when the grouting method is applied in the field, a high injection pressure causes fracturing of the target area and soil. Therefore, the importance of the appropriate injection pressure considering injectability, pore saturation, and stability are emphasized, and it is considered that the results of this study can be used as fundamental data for the development of biopolymer grout materials.

Acknowledgments

This work was supported by a National Research Foundation of Korea (NRF) grant funded by the Korean government. (MSIT) (2020R1A2C1012352).

References

Ahn, S., Ryou, J.E., Ahn, K., Lee, C., Lee, J.D. and Jung, J. (2020), "Evaluation of dynamic properties of sodium-alginate-reinforced soil using a resonant-column test", *Materials*, **14**(11), 2743. https://doi.org/10.3390/ma14112743.

Amelian, S., Rong, C.R., Kim, Y., Lindemann, M. and Bitar, L. (2022), "Weathering durability of biopolymerized shales and glacial tills", *Geomech. Eng.*, **28**(4), 375-384. https://doi.org/10.12989/gae.2022.28.4.375.

Arab, M.G., Mousa, R.A., Gabr, A.R., Azam, A.M., El-Badawy, S.M. and Hassan, A.F. (2019), "Resilient behavior of sodium alginate–treated cohesive soils for pavement applications", *J. Mater. Civ. Eng.*, **31**(1), 04018361. https://doi.org/10.1061/(asce)mt.1943-5533.0002565.

Ayeldeen, M.K., Negm, A.M. and El-sawwaf. M.A. (2016). "Evaluating the physical characteristics of biopolymer/soil mixtures", *Arab J Geosci.*, **9**, 371. https://doi.org/10.1007/s12517-016-2366-1.

Bouazza, A., Gates, W.P. and Ranjith, P.G. (2009), "Hydraulic conductivity of biopolymer-treated silty sand", *Géotechnique*, **59**(1), 71-72. https://doi.org/10.1680/geot.2007.00137.

Butler, M. (2016), Xanthan gum: applications and research studies. Nova Science Inc, New York, NY, USA.

Cao, S., Bate, B., Hu, J. and Jung, J. (2016a), "Engineering behavior and characteristics of water-soluble polymers: implication on soil remediation and enhanced oil recovery", *Sustainability*, **8**(3), 205. https://doi.org/10.3390/su8030205.

Cao, S.C., Dai, S. and Jung, J. (2016b), "Supercritical CO2 and brine displacement in geological carbon sequestration: Micromodel and pore network simulation studies", *Int. J. Greenh. Gas Control.*, **44**, 104-114. https://doi.org/10.1016/j.ijggc.2015.11.026.

Casson, N. (1959), "A flow equation for pigment-oil suspensions of the printing ink type", (Ed., Mills, C.C.), Rheology of Disperse Systems. Pergamon Press, Oxford, 84-104.

Chang, I. and Cho, G.C. (2014), "Geotechnical behavior of a beta-1,3/1,6-glucan biopolymer-treated residual soil", *Geomech.*

Eng., **7**(6), 633-647. https://doi.org/10.12989/gae.2014.7.6.633.

Chang, I., Im, J., Prasidhi, A.K. and Cho, G.C. (2015a), "Effects of Xanthan gum biopolymer on soil strengthening", *Constr. Build. Mater*., **74**, 65-72. https://doi.org/10.1016/j.conbuildmat.2014.10.026.

Chang, I., Lee, M., Tran, A.T.P., Lee, S., Kwon, Y.M. Im, J. and Cho, G.C. (2020), "Review on biopolymer-based soil treatment (BPST) technology in geotechnical engineering practices", *Transp. Geotech*., **24**, 100385.

Chang, I., Prasidhi, A.K., Im, J. and Cho, G.C. (2015b), "Soil strengthening using thermo-gelation biopolymers", *Constr. Build. Mater.*, **77**, 430-438. https://doi.org/10.1016/j.conbuildmat.2014.12.116.

Cheng, Z. and Geng, X. (2021), "Soil consistency and interparticle characteristics of various biopolymer types stabilization of clay", *Geomech. Eng*., **27**(2), 103-113. https://doi.org/10.12989/gae.2021.27.2.103.

Cross, M.M. (1979). "Relation between viscoelasticity and shear-thinning behaviour in liquids", *Rheol Acta*, **18**(5), 609-614. https://doi.org/10.1007/bf01520357.

Fatehi, H., Abtahi, S.M., Hashemolhosseini, H. and Hejazi, S.M. (2018), "A novel study on using protein based biopolymers in soil strengthening", *Constr. Build. Mater*., **167**, 813-821. https://doi.org/10.1016/j.conbuildmat.2018.02.028.

Ham, S.-M., Chang, I., Noh, D.H., Kwon, T.H. and Muhunthan, B. (2018), "Improvement of Surface Erosion Resistance of Sand by Microbial Biopolymer Formation", *J. Geotech. Geoenviron. Eng.*, **144**(7), 06018004. https://doi.org/10.1061/(asce)gt.1943-5606.0001900.

He, Z., Li, Q., Wang, J., Yin, N., Jiang, S. and Kang, M. (2016), "Effect of silane treatment on the mechanical properties of polyurethane/water glass grouting materials", *Constr. Build. Mater.*, **116**, 110-120. https://doi.org/10.1016/j.conbuildmat.2016.04.112.

Hwang, S.P., Yoo, W.K. and Kim, C.Y. (2018), "Experimental Study on Characteristics of Penetration into Microcrack Depending on Viscosity", *Int. J. Struct. Civ. Eng. Res*., **7**(3), 227-232. https://doi.org/10.18178/ijscer.7.3.227-232.

Jang, J., Lee, J. and Jung, J. (2017), "Characterization of Agar for Soil Remediation", *J. Korean Soc. Hazard Mitig*., **17**(6), 351-358. https://doi.org/10.9798/KOSHAM.2017.17.6.351.

Jeoung, J.H., Hwang, S.P., Lee, J.H. and Lee, T.H. (2016), "The study on evaluation of injection performance in micro crack depending on viscosity of grouting material", *J. Korean Soc. Hazard Mitig*., **16**(5), 239-245. https://doi.org/10.7843/kgs.2017.33.9.23.

Jung, J. and Ahn, J. (2014), "Characteristerization of biopolymer solution used for soil remediation and petroleum production", *J. Korean Soc. Hazard Mitig*., **14**(5), 109-114. https://doi.org/10.9798/KOSHAM.2014.14.5.109.

Jung, J., Jang, J. and Ahn, J. (2016), "Characterization of a polyacrylamide solution used for remediation of petroleum contaminated soils", *Materials*, **9**(1), 16. https://doi.org/10.3390/ma9010016.

Karol. R.H. (2003), Chemical Grouting and Soil Stabilization, (1st Edition), CRC Press, Boca Raton, FL, USA.

Ko, D. and Kang, J. (2020), "Biopolymer-reinforced levee for breach development retardation and enhanced erosion control", *Water*, **12**(4), 1070. https://doi.org/10.3390/w12041070.

Kumar, S.A. and Sujatha, E.R. (2021), "Experimental investigation on the shear strength and deformation behaviour of xanthan gum and guar gum treated clayey sand", *Geomech. Eng.*, **26**(2), 101-115. https://doi.org/10.12989/gae.2021.26.2.101.

Lee, M., Im, J., Chang, I. and Cho, G.C. (2021), "Evaluation of Injection capabilities of a biopolymer based grout material", *Geomech. Eng*., **25**(1), 31-40. https://doi.org/10.12989/gae.2021.25.1.031.

Lee, S., Chang, I., Chung, M.K., Kim, Y. and Kee, J. (2017), "Geotechnical shear behavior of Xanthan Gum biopolymer treated sand from direct shear testing", *Geomech. Eng*., **12**(5), 831-847. https://doi.org/10.12989/gae.2017.12.5.831.

Lenormand, R. and Zarcone, C. (1989), "Capillary fingering Percolation and fractal dimension", *Transp. Porous Media*, **4**, 599-612. https://doi.org/10.1007/BF00223630.

Ostwald, W. (1929), "Über die rechnerische Darstellung des Strukturgebietes der Viskosität", *Kolloid-Z*., **47**(2), 176-187. https://doi.org/10.1007/BF01496959.

Park, S.S., Woo, S.W., Jeong, S.W. and Lee, D.E. (2020), "Durability and strength characteristics of casein-cemented sand with sslag", *Materials*, **13**(14), 3182. https://doi.org/10.3390/ma13143182.

Pathak, T.S., Kim, J.S., Lee, S.J., Baek, D.J. and Paeng, K.J. (2008), "Preparation of alginic acid and metal alginate from algae and their comparative study", *J. Polym. Environ.*, **16**, 198-204. https://doi.org/10.1007/s10924-008-0097-4.

Sisko, A.W. (1958), "The flow of lubricating greases", *Ind. Eng. Chem.*, **50**(12), 1789-1792. https://doi.org/10.1021/ie50588a042.

Sochi, T. (2010). "Pore-scale modeling of non-Newtonian flow in porous media", Ph.D. Dissertation, Imperial College London, London.

Soldo, A. and Miletic, M. (2019). "Study on shear strength of Xanthan gum-amended soil", *Sustainability*, **11**(21), 6142. https://doi.org/10.3390/su11216142.

Spariharjaona, A., Eswaran, P., Joel, B.A. and Rajalingam, S. (2019), "Static dissolution-induced 3D pore network modification and its impact on critical pore attributes of carbonate rocks", *Petroleum Exploration and Development*, **46**(2), 374-383. https://doi.org/10.1016/S1876-3804(19)60017-0.

Taytak, B., Pulat, H.F. and Yukselen-Aksoy, Y. (2012). "Improvement of engineering properties of soils by biopolymer additives", *Proceedings of the 3rd International Conference on New Developments in Soil Mechanics and Geotechnical Engineering*, North Cyprus, Turkey, June.

Wiszniewski, M. and Cabalar, A.F. (2014), "Hydraulic conductivity of a biopolymer treated sand", *Proceedings of the 3rd Geotechnical International Conference*, Shanghai, China, May.

Zhang, Q., Hu, X.M., Wu, M.Y., Zhao, Y.Y. and Yu, C. (2018), "Effects of different catalysts on the structure and properties of polyurethane/water glass grouting materials", *J. Appl. Polym. Sci*., **135**(27), 46460. https://doi.org/10.1002/app.46460.

Zhou, F., Sun, W., Shao, J., Kong, L. and Geng, X. (2020). "Experimental study on nano silica modified cement base grouting reinforcement materials", *Geomech. Eng*., **20**(1), 67-73. https://doi.org/10.12989/gae.2020.20.1.067.